ChemPubSoc Europe

DOI: 10.1002/celc.201600875

CHEMELECTROCHEM Articles

Towards Higher Energy Density Redox-Flow Batteries: Imidazolium Ionic Liquid for Zn Electrochemistry in Flow Environment

Kalani Periyapperuma,[a] Yafei Zhang,[a] Douglas R. MacFarlane,[b] Maria Forsyth,[a] Cristina Pozo-Gonzalo,[a] and Patrick C. Howlett*[a]

We present the first demonstration of an ionic liquid electrolyte under a realistic flow environment for applications in redox-flow batteries based on the Zn^{2+}/Zn^0 redox couple. An electrolyte mixture containing $Zn(dca)_2$ and 3 wt% H_2O in 1-ethyl-3-methylimidazolium dicyanamide, [Emim][dca], ionic liquid was used to study the effects of Zn^{2+} concentration and flow rate on the Zn^{2+}/Zn^0 electrochemical performance as well as its impact on the morphology of the Zn deposit. An optimized Zn^{2+} concentration and flow rate were determined by using an in-house-designed 3D-printed flow-cell prototype. Surface characterization through SEM revealed that both the concentration and flow rate directly impact Zn morphology under flow conditions. The electrolyte mixture with a higher $Zn(dca)_2$ concentration (18 mol%) showed favourable results; voltammetry showed higher peak current densities (100 mA/cm^2 discharge current density) and more positive Zn electrodeposition potentials (−1.33 V vs Ag/AgOTf) coupled with higher cycling efficiency (45±3%) compared to those obtained with the lower Zn concentration system (9 mol%, −1.44 V vs Ag/AgOTf, 48 mA/cm^2 discharge current density and 33±3% cycling efficiency).

1. Introduction

With continuous increase in global energy demand, developing efficient and cost-effective rechargeable energy-storage devices has become crucial. In the quest for next-generation rechargeable battery technologies, redox flow batteries (RFBs) have been extensively investigated for medium- to large-scale energy storage applications because of their cost effectiveness, mobility, flexibility in terms of independent control of power output and energy capacity and safety advantages over current state-of-the-art Li-ion batteries.[1–4]

Zinc is an attractive anode material for RFBs owing to its high negative potential, high theoretical energy density, low material cost, abundant supply and environmental friendliness.[5] In the past, rechargeable RFBs based on Zn coupled with different electropositive redox species including nickel, manganese dioxide, chlorine, bromine, cerium and ferricyanide have been investigated to achieve high energy density.[6–9] Among these, Zn–Br is one of the most developed Zn RFB owing to its high theoretical energy density (440 Wh Kg^{-1}), theoretical cell potential of 1.82 V, good reversibility and relatively cheap materials.[1,3] This system has been reported to have a cycling efficiency of 75–80%.[10] However, Zn–Br RFBs are limited by material corrosion and Zn dendrite formation.[3]

The Zn–Ce RFB is also promising, with a high cell potential of 2.4 V and high discharge current densities of 400–500 mA/cm^2. However, these cells require high concentrations of corrosive supporting electrolyte, methanesulfonic acid, to increase the solubility of Ce salt; this has a negative impact on the Zn electrode and increases parasitic H_2 gas evolution resulting in relatively low cycle life (<25 cycles).[1,5,11] These issues involving safety and the corrosive nature of the electrolyte are not limited to Zn-based RFBs but also occur with other redox flow chemistries, including all-vanadium RFBs, which use highly corrosive sulfuric acid as the supporting electrolyte. Ionic liquids (ILs) are promising safer and less corrosive solvents because of their high thermal and electrochemical stability, wide electrochemical windows and negligible vapour pressures.

Recent studies have shown reversible Zn electrodeposition and dissolution in IL-based electrolytes.[12,13] Among ILs, those containing dca^- anions exhibit low viscosities at room temperature, implying efficient mass transport and higher conductivity for electrochemical applications.[14] Previously, our group has investigated the role of added Zn^{2+} salt and the effects of water content on Zn electrochemical performance and deposition morphology in [Emim][dca] in IL electrolyte under static (i.e., 'no flow') conditions.[15] It was concluded that electrolyte system based on $Zn(dca)_2$ salt is most appropriate due to its lower onset potential of −1.8 V vs $Fc^{0/+}$ for Zn deposition, which is the result of weaker metal anion interactions, and higher current densities for Zn deposition/dissolution (70/

[a] K. Periyapperuma, Dr. Y. Zhang, Prof. M. Forsyth, Dr. C. Pozo-Gonzalo, Prof. P. C. Howlett
ARC Centre of Excellence for Electromaterials Science (ACES)
Institute for Frontier Materials (IFM)
Deakin University
75 Pigdons Road, Waurn Ponds
Victoria 3216 (Australia)
E-mail: patrick.howlett@deakin.edu.au
[b] Prof. D. R. MacFarlane
ARC Centre of Excellence in Electromaterials Science
School of Chemistry
Monash University
Wellington Road, Clayton, 3800 (Australia)

Supporting information for this article is available on the WWW under http://dx.doi.org/10.1002/celc.201600875

40 mA/cm^2) compared to Cl^-, SO_4^{2-} and acetate based Zn salts.[12] Adding 3 wt% H_2O to the [Emim][dca] IL electrolyte containing $Zn(dca)_2$ has facilitated smoother deposition of Zn with closely-packed needle-like morphology and good adhesion to the GC electrode. Although $Zn(dca)_2$ in [Emim][dca] IL with 3 wt% H_2O has shown great promise in regard to Zn rechargeable batteries, their application under flow configuration is yet to be reported.

Furthermore, it has been reported that the morphologies of Zn deposits are directly correlated with operating conditions such as the additives used, cycling temperatures, applied current densities and flow velocities.[16–19] Since most of these studies were performed either under static conditions and/or using aqueous electrolyte systems, a knowledge gap exists in understanding how ILs can affect the morphology of Zn deposited under flow conditions. Because the morphology can affect the cycling performance and ultimately the coulombic efficiency of the battery, it is important to understand this effect.[18]

To the best of our knowledge, although there are multiple reports of Zn electrochemistry in ionic liquids, it has not yet been evaluated under flow conditions. In our current work, we assess the effects of Zn^{2+} concentration and flow rate of electrolyte on electrochemical performance and morphology of Zn deposited using the previously mentioned electrolyte system containing various concentrations of $Zn(dca)_2$ in [Emim][dca] IL and 3 wt% water. Unlike most previous studies on flow batteries,[20–22] here we were able to reduce the volume of electrolyte required per test to 4 mL. The electrochemical performance under flow conditions was measured in a 3D-printed flow half-cell prototype designed in-house.

2. Results and Discussion

In this study we investigated the electrochemistry and morphology of Zn focused on two main aspects: (1) effect of Zn^{2+} concentration on Zn electrochemistry and morphology under static, stirring and flow conditions, (2) effect of flow rate on Zn electrochemistry and morphology. The cycling efficiencies obtained under static, stirring and flow environments are summarized in Table 1, and will be discussed in detail later in this section.

Table 1. Summary of cycling efficiencies obtained with 9 mol% and 18 mol% $Zn(dca)_2$ + [Emim][dca] + 3 wt% H_2O under static, stirring and flow conditions at ±3 mA/cm^2

Electrolyte	Static in a standard cell vial [%]	Stirring in a standard cell vial[a] [%]	Flow in flow cell setup[b] [%]
9 mol%	82±3	67±3	33±3
18 mol%	84±3	68±3	45±3

[a] At 320 rpm. [b] 11 mL/min.

2.1 Effect of Salt Concentration on Zn^{2+}/Zn^0 Electrochemistry and Morphology under Stirring Conditions

Figure 1 shows the cycling performance of 9 mol% and 18 mol% $Zn(dca)_2$ electrolyte mixtures cycled in a standard cell

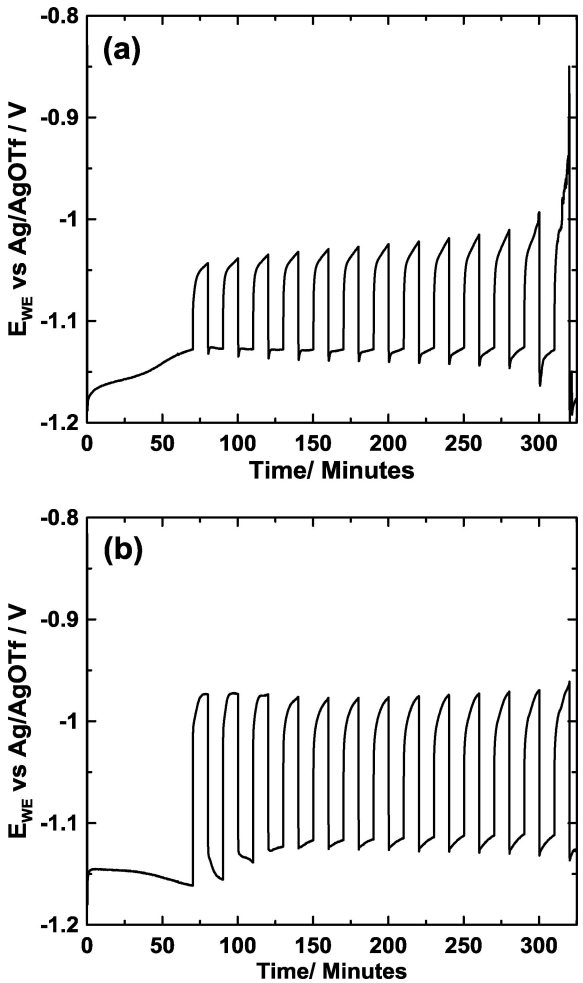

Figure 1. Chronopotentiograms of [Emim][dca] + 3 wt% H_2O + a) 9 mol% $Zn(dca)_2$ and b) 18 mol% $Zn(dca)_2$ stirring at 320 rpm in a standard cell vial at an applied current density of ±3 mA/cm^2.

vial, while stirring the electrolyte at 320 rpm. Stirring creates a flow environment around the electrodes similar to that in the flow-cell setup used in our study. The initial 1 hour excess plated charge deposition of Zn on GC electrode surface at a constant current density of ±3 mA/cm^2 creates an initial deposit suitable for subsequent 'cycling'. The cell was then cycled at 10 minute step times until cell failure. This is a well-established method to measure the average cycling efficiency of energy-storage electrodes.[23,24] The 9 mol% $Zn(dca)_2$ mixture shows an initial charging potential, which gradually increases up to −1.13 V while 18 mol% $Zn(dca)_2$ maintains a fairly stable potential under the same conditions. In both electrolyte mixtures, Zn is electrodeposited at a potential of −1.08 V. As shown in Figure 1(b), the higher overpotential observed with 18 mol% $Zn(dca)_2$ could be a result of increased viscosity of the

solution at high Zn^{2+} salt concentration.[25] Both electrolyte mixtures yielded similar cycling efficiencies of 68±3%. The average cycling efficiencies were calculated using Equation (1), where N is the number of cycles, Q_{ex} is excess plated charge and Q_{ps} is cycled charge.

$$CE = 100^{*}NQ_{ps}/(NQ_{ps} + Q_{ex}) \quad (1)$$

where N is the number of cycles, Q_{ex} is excess plated charge and Q_{ps} is cycled charge.

The sharp increase in voltage at the end of the final cycle is caused by complete consumption of the initial excess Zn deposit. This experiment demonstrates that the electrolyte mixture comprising [Emim][dca] with $Zn(dca)_2$ and 3 wt% H_2O can support continual Zn electrodeposition and dissolution under stirring.

To study the effects of Zn concentration on electrodeposited Zn morphology under stirring conditions, Zn was plated onto a GC electrode surface from 9 mol% and 18 mol% $Zn(dca)_2$ electrolyte mixtures for 1 hour at a constant current density of ±3 mA/cm^2 at 320 rpm, and micrographs of the Zn deposits obtained are shown in Figures 2(a) and (b), respectively. As shown in Figure 2(a), the less concentrated electrolyte

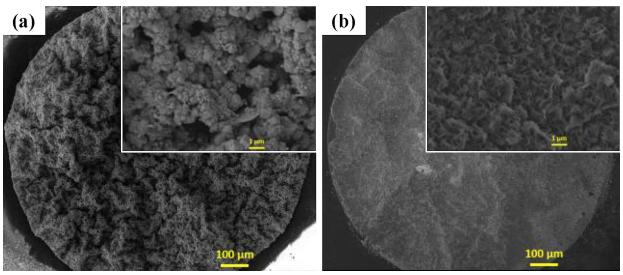

Figure 2. SEM images of Zn deposits after 1 h of electrodeposition from either a) 9 mol% $Zn(dca)_2$ or b) 18 mol% $Zn(dca)_2$ + [Emim][dca] + 3 wt% H_2O stirring at 320 rpm at an applied current density of −3 mA/cm^2. (insets: 1 µm scale, others 100 µm scale).

resulted in a non-uniform, porous deposit with cubic grains. The more concentrated system yielded a smoother Zn deposit with closely-packed needle-like morphology.

The morphologies of Zn deposited under static conditions from [Emim][dca] containing 9 mol% (Figure 3a) and 18 mol% (Figure 3b) $Zn(dca)_2$ at −3 mA/cm^2 were also compared. Similar to the results obtained under stirring, different Zn^{2+} concentrations resulted in distinct Zn morphologies. The deposit from the 9 mol% electrolyte mixture was mostly small grains, along with horizontally-grown feather-like Zn structures. Previously, our group has studied the morphology of Zn using a similar electrolyte mixture with 9 mol% $Zn(dca)_2$ under static condition, but at different current densities and deposition potentials under an inert gas environment.[12,15] Under these conditions, spherical nuclei were observed consisting of Zn needles fused together to form a smooth deposit. As shown in Figure 3(b), the 18 mol% electrolyte mixture yielded a Zn deposit comprising aggregates of small spheres with needle-

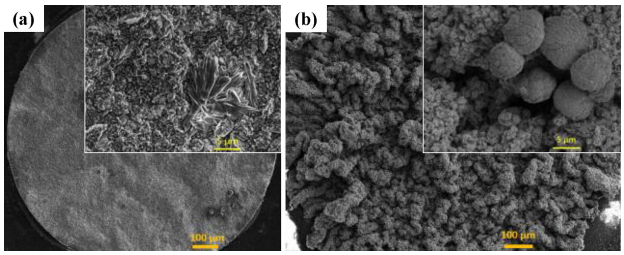

Figure 3. SEM images of Zn deposits after 1 h at an applied current density of −3 mA/cm^2 in static [Emim][dca] + 3 wt% H_2O containing either a) 9 mol% $Zn(dca)_2$ or (b) 18 mol% $Zn(dca)_2$.

like morphology, along with 5 µm or bigger spheres displaying a different morphology. In contrast to the stirring experiment, here the Zn deposit is porous and non-uniform with the 18 mol% electrolyte mixture compared to 9 mol%.

This indicates that the flow environment has facilitated formation of a uniform Zn deposit at higher redox active species concentration. A uniform Zn deposit is critical in obtaining a less dendritic surface, one of the key challenges yet to be overcome in Zn-based RFBs with aqueous electrolytes.[18] As described in the literature, operating conditions such as current density, electrode surface and experimental environment have significant effects on Zn morphology.[19] The uniform deposit obtained with the [Emim][dca] IL-based electrolyte mixture containing 18 mol% $Zn(dca)_2$ is a promising step towards this goal. In summary, the more concentrated electrolyte showed favourable results under stirring, resulting in a more uniform deposit compared to that obtained under static conditions. To further investigate the effect of concentration on Zn electrochemical performance and morphology under flow conditions, these electrolyte systems were then tested in our in-house designed flow half-cell.

2.2 Effect of Concentration on Zn Electrochemistry and Morphology under Flow Conditions

With continuous development in research tools, 3D printing has become an approachable and affordable method for rapid manufacturing of cell prototypes and cell components, even those with a high degree of complexity.[22] This has been particularly advantageous for our early stages of small-scale redox flow-battery development work, which often demands flexibility in cell design. Figure 4 shows a schematic cross section of the 3D-printed flow half-cell prototype used in this study (the cell body is 20×45 mm). The electrolyte is pumped through the channel in the printed cell body by a peristaltic pump, and undergoes electron-transfer reactions at the WE and CE during charging and discharging processes. The surfaces of the RE, WE and CE, placed in the corresponding sleeves, sit parallel to the electrolyte flow to avoid possible turbulence around the electrodes. This cell setup was used to study the Zn electrochemistry and morphology under flow conditions at different Zn^{2+} concentrations and flow rates.

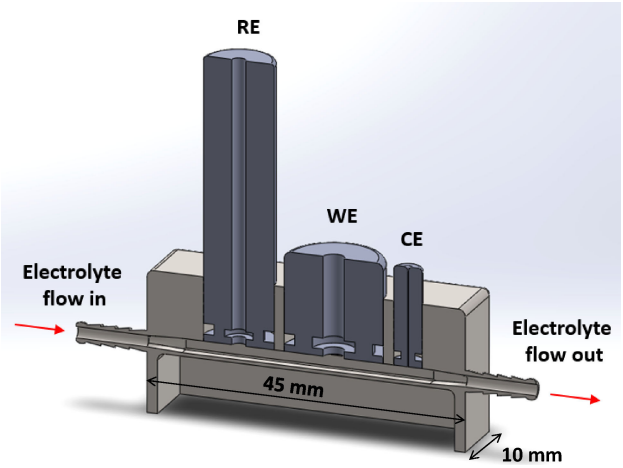

Figure 4. Schematic cross section of the flow half-cell design used in this study.

Figure 5 presents the cyclic voltammograms obtained for the 9 mol% and 18 mol% $Zn(dca)_2$ electrolyte mixtures at

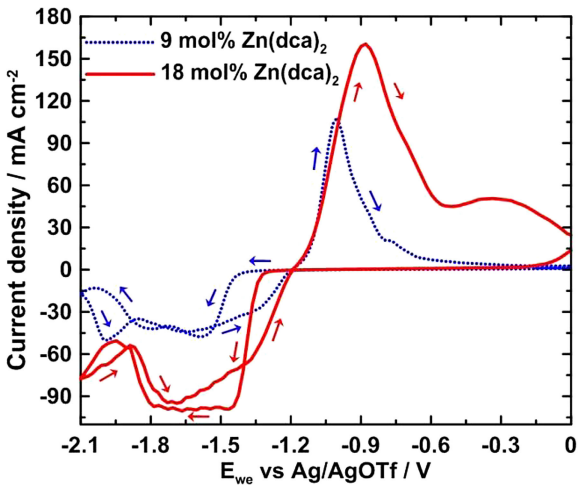

Figure 5. Cyclic voltammograms for [Emim][dca] + 3 wt% H_2O with different concentrations of $Zn(dca)_2$. Scan rate 100 mV/s, flow rate 22 mL/min, 2nd scan.

22 mL/min flow rate. The first reduction peak obtained with 9 mol% $Zn(dca)_2$ at an onset potential of −1.44 V corresponds to Zn electrodeposition, with a peak current density of *ca.* 48 mA/cm^2 at −1.58 V. When the concentration of Zn^{2+} is increased to 18 mol%, the onset of Zn reduction occurs at a less negative potential, −1.33 V, possibly because of a different speciation mechanism at higher concentrations. The significantly higher peak current density of *ca.*100 mA/cm^2 obtained at −1.46 V with 18 mol% $Zn(dca)_2$ is generated by the higher Zn^{2+} concentration that facilitates the reaction at the electrode interface. These current densities obtained under flow are higher than those recorded in the literature under static condition with similar electrolyte mixtures containing 10 and 20 mol% $Zn(dca)_2$.[26] Although the 20 mol% system gave greater current densities than the 10 mol% system for Zn plating and stripping under static conditions, the Zn electrodeposition potential was more negative. In contrast, under flow, the more concentrated electrolyte mixture containing 18 mol% $Zn(dca)_2$ gives both superior peak current densities and a less negative Zn electrodeposition potential than the 9 mol% system. The deposition overpotential is clearly dependent upon the Zn^{2+} concentration, but the origin of the different behaviour under flow is less obvious. Notably, our recent surface studies have shown the dominant role of ion arrangements at the electrode surface in dictating the Zn deposition potential in these Zn-IL-H_2O systems.[27]

For both concentrations, a second reduction peak occurs when the reduction is extended to −2.1 V. As mentioned in the literature,[26] two reduction peaks might result from two distinct morphologies or structures of Zn being deposited onto the GC electrode surface. It is also possible for the second reduction peak to be associated with the reduction of the imidazolium cation or water, as the negative scan is approaching the reduction limit of the IL with 3 wt% water (−2.25 V in Figure 7a).[12] Nevertheless, no change in colour or bubble formation was detected in the electrolyte solution during or after the experiment. At both concentrations, the oxidation of reduced Zn begins at −1.14 V. The oxidation peak current densities also increase with increasing redox couple concentration following the same trend during the negative scan, suggesting that the Zn deposits readily oxidise into the solution.

The morphologies of the Zn electrodeposits were compared using optical profilometry and SEM, as shown in Figure 6. The

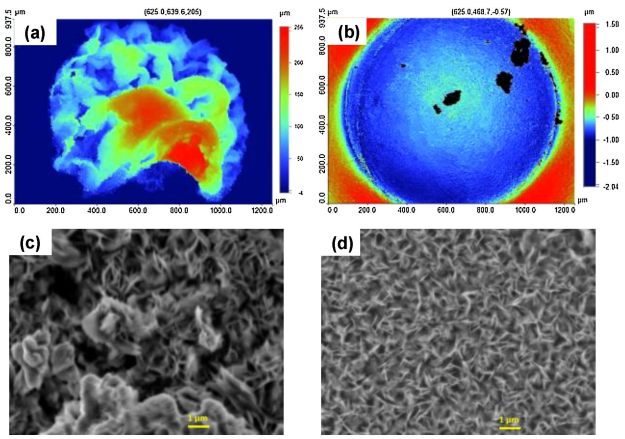

Figure 6. Profilometric images of Zn deposits after 1 h in [Emim][dca] + 3 wt% H_2O + a) 9 mol% $Zn(dca)_2$, and b) 18 mol% $Zn(dca)_2$, at 22 mL/min flow rate and −3 mA/cm^2 current density; (c, d) corresponding SEM images. The black spots in (b) are out-of-scale Zn deposits.

uniformity of Zn deposits were determined by optical microscopy by measuring the deposit thickness indicated by different colours within the circular GC electrode as shown in Figure 8(a–b). A monochromatic colour similar to Figure 8b represents a uniform surface with even deposit thickness. Zn deposited from 9 mol% $Zn(dca)_2$ is non-uniform and porous, similar to that

obtained from the same mixture under stirring. In contrast, a closely packed, uniform Zn deposit was obtained in the electrolyte with 18 mol% $Zn(dca)_2$ under flow. This improved uniformity with higher $Zn(dca)_2$ concentration was also seen under stirring. This is important to help obtain less dendritic electrodeposits, and avoid short circuits and safety issues in RFBs. The electrolyte mixture containing 18 mol% $Zn(dca)_2$ was chosen for further studies because of its superior Zn plating/stripping current densities, less negative Zn electrodeposition potential and the uniform Zn deposit obtained in the above experiment.

2.3 Effect of Flow Rate on Zn Electrochemistry and Morphology under Flow Conditions

To study the effect of flow rate on Zn electrodeposition/dissolution potentials and resulting current densities, cyclic voltammetry was performed on the electrochemical system at different flow rates. Figure 7 shows the cyclic voltammograms for [Emim][dca] containing 18 mol% $Zn(dca)_2$ and 3 wt% H_2O at 6, 13, 22 and 40 mL/min flow rates. The stability of the IL with 3 wt% H_2O (i.e., without Zn salt) was measured under flow condition at 6 mL/min flow rate as a control experiment (Figure 7a); the neat IL was reductively stable until −2.25 V. In Figure 7b–e the peak current density for Zn electrodeposition and dissolution increases with increasing flow rate. This is attributed to the increase in mass transfer with increasing flow rate.[28]

The onset of Zn electrodeposition in this system occurs at −1.3 V, is independent of the flow rate. In addition, a second reduction peak was observed at −2.1 V at all flow rates. This resembles the peak which occurs under static condition in a similar electrolyte mixture, close to the reduction limit of the solvent.[26] As mentioned before, this peak might be a result of either another distinct morphology of Zn being deposited onto the GC electrode surface, or possibly the reduction of imidazolium cation or water, as the negative scan is approaching the reduction limit of IL with 3 wt% water (−2.25 V in Figure 7a). As in the previous experiment (Figure 5), neither change in colour, nor bubble formation was detected in the electrolyte solution during or after the experiment. The peak potential for the oxidation process corresponding to Zn dissolution was observed at −0.9 V at all flow rates.

The effect of flow rate on Zn morphology was investigated at 6, 13 and 22 mL/min flow rates by depositing Zn on GC electrode surface for 1 hour at a constant current density of $-3\ mA\,cm^{-2}$ using chronopotentiometry. At 6 mL/min (Figure 8a) the Zn deposit shows a highly crystalline needle-like structure, whereas 13 mL/min flow rate (Figure 8b) led to a deposit of thin plates arranged perpendicular to the electrode surface. The morphology of Zn deposited at 13 mL/min is quite similar to that obtained at 22 mL/min (Figure 5d), except the latter was a more compact deposit. These results indicate that the lower and higher flow rates significantly alters the morphology of Zn deposit. Flow rates above 22 mL/min were not examined due to limitations of the apparatus. Since similar Zn morphologies were obtained for 11 (Figure S1-d), 13 and 22 mL/min flow rates, 11 mL/min was chosen for further experiments.

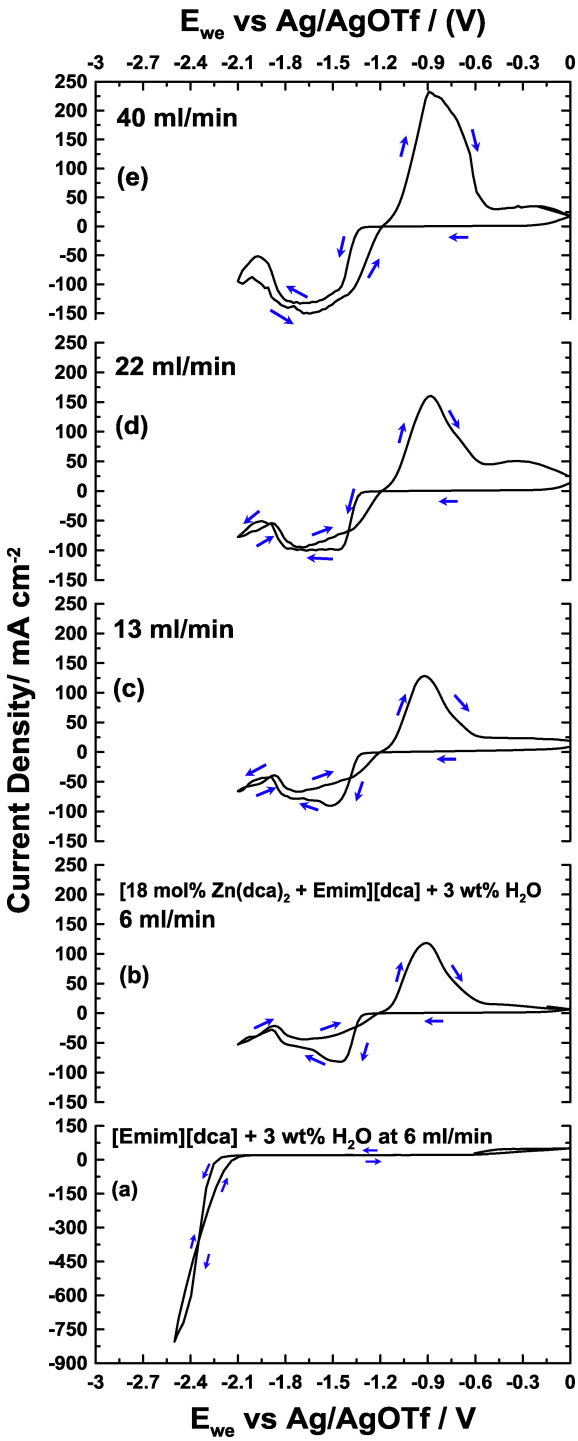

Figure 7. Cyclic voltammograms for a) neat [Emim][dca] + 3 wt% H_2O at 6 mL/min; [Emim][dca] with 3 wt% H_2O and 18 mol% $Zn(dca)_2$ at b) 6 mL/min, c) 13 mL/min, d) 22 mL/min, and e) 40 mL/min flow rates (scan rate 100 mV/s).

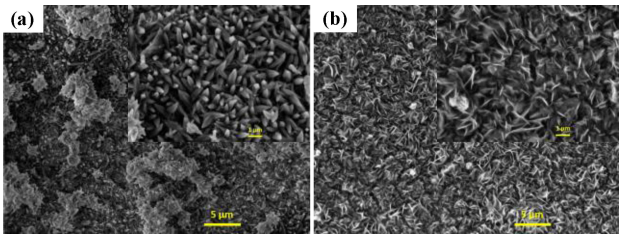

Figure 8. SEM images of Zn deposits after plating Zn for 1 h from 18 mol% $Zn(dca)_2$ + [Emim][dca] + 3 wt% H_2O flowing at a) 6 mL/min and b) 13 mL/min rates and −3 mA/cm^2 current density. (inset: 1 µm scale, others 5 µm scale).

2.4 Effect of Concentration on Cycling Performance under Flow Conditions

The cycling performance of electrolyte systems containing 9 mol% or 18 mol% $Zn(dca)_2$ was measured at 11 mL/min flow rate at an applied current density of −3 mA/cm^2, as shown in Figure 9(a) and (b). The increase in Zn electrodeposition potential with increased cycling at both concentrations is attributed to modification of the working electrode surface caused by Zn plating and stripping. Irrespective of the higher overpotential, 18% $Zn(dca)_2$ resulted in better cycling efficiency (46 ± 3% compared to 33 ± 3% for 9% $Zn(dca)_2$). This difference may be a result of increased flux of Zn^{2+} ions to the GC electrode surface at higher concentration as well as the distinctive Zn morphologies obtained at the different concentrations, as shown in Figure S1.

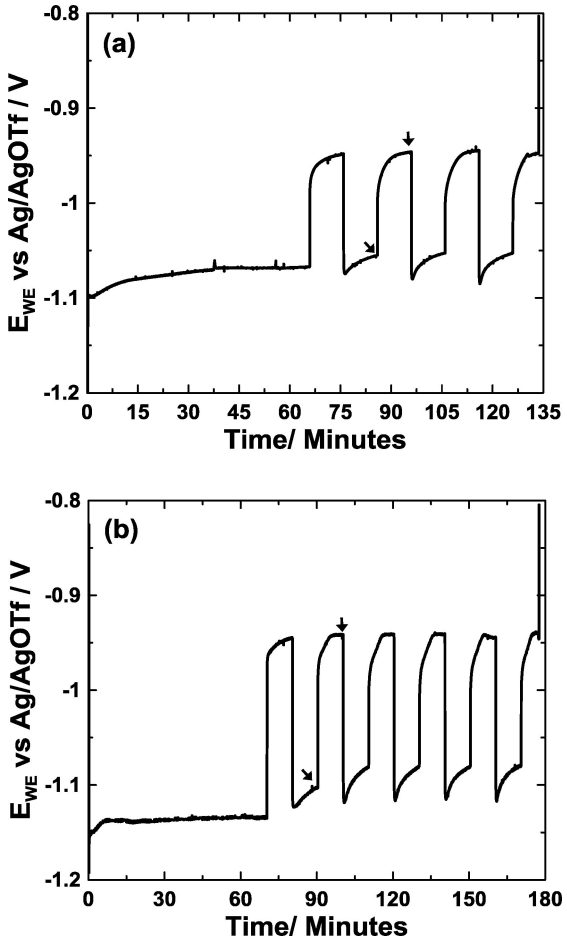

Figure 9. Chronopotentiograms in [Emim][dca] with 3 wt% H_2O with a) 9 mol% $Zn(dca)_2$ or b) 18 mol% $Zn(dca)_2$ at an applied current density of ±3 mA/cm^2. Arrows indicate sampling points for SEM imaging presented in Figure S1.

The effect of concentration on Zn morphology at 11 mL/min flow rate as well as the change in morphology during cycling at each concentration was also studied. In Figure S1 (a-f) we show the morphologies of Zn deposits obtained from 9 mol% and 18 mol% $Zn(dca)_2$ electrolyte mixtures after plating Zn for 1 hour, after the 2nd charge and discharge cycles (indicated by arrows in Figure 9). With 9 mol% $Zn(dca)_2$, a non-uniform, porous Zn deposit was obtained after depositing Zn for 1 hour. As shown in Figure S1(a) inset, the deposit has a platelet-like morphology similar to that reported in the literature,[12] and with cycling, the grain size becomes smaller. With 18 mol% $Zn(dca)_2$, a more uniform deposit was obtained after plating Zn for 1 hour. No significant change in morphology was detected after cycling, except the grain size was smaller after the 2nd discharge cycle (Figure S1-f). Furthermore, patches of GC electrode surface appeared after the 2nd discharge where Zn had been completely removed. The EDX analysis of the electrodeposit at a low accelerating voltage, 5 kV, revealed that the surface of the Zn deposit is completely oxidized as a consequence of cycling in air (atomic percentages: 26.76% O and 25.68% Zn), but at a higher accelerating voltage of 10 kV, which has a larger interaction volume and probes deeper into the sample, an increased atomic percentage of Zn was noted compared to oxygen (atomic percentages: 20.17% O and 32.73% Zn).

Surprisingly, the cycling efficiency (CE) values obtained from Equation (1) with 9 mol% and 18 mol% $Zn(dca)_2$ in the flow cell setup are lower than those obtained under stirring at 320 rpm in a standard cell vial, as summarised in Table 1.

As shownin Table 1, stirring in a standard cell vial has reduced the CE compared to the values obtained under static conditions at both concentrations. Whilst different cell configurations might be a possible contributor for this difference, the exact reason is not yet clear. A more significant difference in efficiency was noted in the experiments performed in the flow cell setup compared to the stirring condition at 320 rpm. When the cycle performance of 18 mol% $Zn(dca)_2$ electrolyte mixture was measured under static condition in our flow cell setup, the efficiency obtained was also only 45 ± 3% (not shown), whereas in the standard cell vial 84 ± 3% efficiency was obtained. This indicates that the flow cell geometry used here limits the maximum efficiency to 45 ± 3%. This disparity in the performance suggests that further improvement in cycling can be achieved with optimized cell configuration.

3. Conclusions

We have investigated [Emim][dca] IL with added $Zn(dca)_2$ as a potential electrolyte for Zn-based redox flow batteries. When the Zn^{2+} concentration increased to 18 mol%, the Zn electrodeposition and dissolution peak current densities increased, while the Zn deposition potential shifted to more positive values under flow. The increase in current density was attributed to the increased redox couple concentration available for reduction at the working electrode surface. The shift in Zn electrodeposition overpotential might be due to speciation mechanisms at different concentrations under flow conditions or the presence of ionic layers at the electrode surface as recently reported,[27] and further studies are required to investigate this phenomena. The effect of flow rate on Zn electrochemistry was also investigated in this study. Increasing flow rate increased the Zn plating and stripping current densities by increasing the mass transfer rate. Finally, surface characterization revealed that the Zn morphology can be controlled via the concentration of Zn^{2+} in the electrolyte mixture and the applied flow rate. The electrolyte mixture containing 18 mol% $Zn(dca)_2$ in [Emim][dca] IL showed promising results including superior Zn oxidation/reduction current densities, low overpotentials for Zn electrodeposition, and uniform Zn morphologies under flow conditions. Further optimization of the flow cell configuration is needed to improve cycling performance for redox flow batteries. Therefore, further modifications to the present 3D printed cell design including increasing CE surface area, reducing active species diffusion distance between electrodes are underway.

Experimental Section

[Emim][dca] IL (>98%, Ionic Liquid Technologies) was purified by dissolving in dichloromethane and filtering the resultant cloudy solution through a 0.2 μm Teflon syringe filter.[12] The IL was then dried under vacuum and the water content was measured using a Model 756/831 Karl Fischer Coulometer (MEP Instruments, Australia). The water content of the dried IL was <400 ppm. $Zn(dca)_2$ was synthesized by reacting zinc nitrate hexahydrate (98%, Sigma-Aldrich) and sodium dicyanamide (96%, Sigma-Aldrich) in water at a 1:2 mole ratio at room temperature.[29] The reaction mixture was stirred overnight. The resulting white precipitate was filtered and washed several times with distilled water to remove remaining nitrates and finally dried under high vacuum for 3 days. The purity of $Zn(dca)_2$ solid was tested by both microanalysis (Campbell Microanalytical Laboratory, University of Otago, New Zealand) and EDTA titration. Both the techniques provided compatible results.

Voltammetric experiments were performed on a Biologic VMP3/Z multi-channel potentiostat using a 3-electrode set-up consisting of a 1 mm diameter GC (ALS Co. Ltd, Japan) WE, 0.5 mm diameter Pt (for cyclic voltammetry) or Zn wire (for chronopotentiometry) counter electrode (CE) and Ag/Ag^+ reference electrode (RE) made up of an Ag wire immersed in a 5 mM silver triflate (AgOTf) in [Emim][dca] solution separated from the bulk solution by a porous frit. The redox potential of ferrocene/ferrocenium was +0.44 V vs the Ag/AgOTf reference electrode. All of the potentials in this study are given against this reference electrode unless otherwise stated. The cyclic voltammetry experiments were performed under flow condition within a potential range from 0 V to −2.1 V at 100 mV/s scan rate. The chronopotentiometric measurements were taken at a current density of ±3 mA/cm^2 under static, stirring and flow conditions. The experiments under flow condition were performed in a flow half-cell setup designed in house. This was 3D printed using a UV-cured acrylic material, which is chemically stable towards the IL electrolyte. The electrolyte solutions were pumped into the flow half-cell setup using a peristaltic pump.

The electrolyte solutions were prepared by adding 9 or 18 mol% of $Zn(dca)_2$ salt to [Emim][dca] IL. After taking into account the water content in the IL and Zn^{2+} salt mixture, the total water content was adjusted to 3±0.03 wt% by adding deionised water. All the above experiments were performed at room temperature in open atmosphere. The average cycling efficiencies of the above systems were calculated using Equation (1), where N is the number of cycles, Q_{ex} is excess plated charge and Q_{ps} is cycled charge.

Scanning Electron Microscopy (SEM, JSM IT 300 Series) and Energy Dispersive X-ray Spectroscopy (EDX, Oxford X-Max 50 mm^2 EDX detector) were used to characterize the surface morphology and the composition of Zn deposits. The deposits were gently rinsed with deionised water to remove residual ionic liquid and dried under a stream of N_2 gas prior to insertion in the SEM. Profilometric measurements were taken using a Bruker Contour GT–K1 model profilometer.

Acknowledgements

The authors gratefully acknowledge financial support from the Australian Research Council through the Centre of Excellence for Electromaterials Science (ACES). M. F. and D. R. M. acknowledge the ARC Laureate program. We also thank Shannon Biddulph for assistance in designing and drawing the flow cell setup. This work used the 3D printing facility at Deakin University, Geelong Engineering Campus.

Conflict of Interest

The authors declare no conflict of interest.

Keywords: flow conditions · flow rate · morphology · redox flow · zinc

[1] P. Leung, X. Li, C. P. de Leon, L. Berlouis, C. T. J. Low, F. C. Walsh, *RSC Adv.* **2012**, *2*, 10125–10156.
[2] W. Wang, Q. Luo, B. Li, X. Wei, L. Li, Z. Yang, *Adv. Funct. Mater.* **2013**, *23*, 970–986.
[3] A. Z. Weber, M. M. Mench, J. P. Meyers, P. N. Ross, J. T. Gostick, Q. Liu, *J. Appl. Electrochem.* **2011**, *41*, 1137–1164.
[4] S. Eckroad, *Handbook of Energy Storage for Transmission & Distribution Applications*, **2002**.
[5] P. K. Leung, C. Ponce De Leon, C. T. J. Low, F. C. Walsh, *Electrochim. Acta* **2011**, *56*, 6536–6546.
[6] Y. Ito, M. Nyce, R. Plivelich, M. Klein, D. Steingart, S. Banerjee, *J. Power Sources* **2011**, *196*, 2340–2345.
[7] Y. Ito, M. Nyce, R. Plivelich, M. Klein, S. Banerjee, *J. Power Sources* **2011**, *196*, 6583–6587.
[8] B. D. Sawyer, G. J. Suppes, M. J. Gordon, M. G. Heidlage, *J. Appl. Electrochem.* **2011**, *41*, 543–550.
[9] P. K. Leung, C. Ponce De Leon, C. T. J. Low, A. A. Shah, F. C. Walsh, *J. Power Sources* **2011**, *196*, 5174–5185.

[10] S. Suresh, T. Kesavan, Y. Munaiah, I. Arulraj, S. Dheenadayalan, P. Ragupathy, *RSC Adv.* **2014**, *4*, 37947.
[11] G. L. Soloveichik, *Chem. Rev.* **2015**, *115*, 11533–11558.
[12] T. J. Simons, D. R. Macfarlane, M. Forsyth, P. C. Howlett, *ChemElectroChem* **2014**, *1*, 1688–1697.
[13] M.J. Deng, P.C. Lin, J.K. Chang, J.M. Chen, K.T. Lu, *Electrochim. Acta* **2011**, *56*, 6071–6077.
[14] D. R. MacFarlane, S. A. Forsyth, J. Golding, G. B. Deacon, *Green Chem.* **2002**, *4*, 444–448.
[15] T. J. Simons, A. A. J. Torriero, P. C. Howlett, D. R. MacFarlane, M. Forsyth, *Electrochem. Commun.* **2012**, *18*, 119–122.
[16] M. Xu, D. G. Ivey, W. Qu, Z. Xie, *J. Power Sources* **2015**, *274*, 1249–1253.
[17] Z. Liu, S. Z. El Abedin, F. Endres, *Electrochim. Acta* **2013**, *89*, 635–643.
[18] Z. Liu, T. Cui, G. Pulletikurthi, A. Lahiri, T. Carstens, M. Olschewski, F. Endres, *Angew. Chemie – Int. Ed.* **2016**, *55*, 2889–2893.
[19] A. Gavriloviü-Wohlmuther, A. Laskos, C. Zelger, B. Gollas, A. H. Whitehead, *J. Energy Power Eng.* **2015**, *9*, 1019–1028.
[20] B. Huskinson, M. P. Marshak, C. Suh, S. Er, M. R. Gerhardt, C. J. Galvin, X. Chen, A. Aspuru-Guzik, R. G. Gordon, M. J. Aziz, *Nature* **2014**, *505*, 195–8.
[21] T. Janoschka, N. Martin, U. Martin, C. Friebe, S. Morgenstern, H. Hiller, M. D. Hager, U. S. Schubert, *Nature* **2015**, *527*.
[22] L. F. Arenas, F. C. Walsh, C. P. de León, *ECS J. Solid State Sci. Technol.* **2015**, *4*, 3080–3085.
[23] A. F. Hollenkamp, P. C. Howlett, D. R. MacFarlane, S. A. Forsyth, M. Forsyth, *ENERGY STORAGE DEVICES*, **2009**.
[24] A. F. Hollenkamp, P. C. Howlett, D. R. MacFarlane, S. A. Forsyth, *CONDUCTIVE POLYAMINE-BASED ELECTROLYTE*, **2006**.
[25] Q. Xu, T. S. Zhao, C. Zhang, *Appl. Energy* **2014**, *130*, 139–147.
[26] T. J. Simons, P. C. Howlett, A. A. J. Torriero, D. R. Macfarlane, M. Forsyth, *J. Phys. Chem.* **2013**, *117*, 2662–2669.
[27] S. Begić, H. Li, R. Atkin, A. F. Hollenkamp, P. C. Howlett, *Phys. Chem. Chem. Phys.* **2016**, *Accepted*, DOI 10.1039/c2cp40963a.
[28] R. Bertazzoli, C. A. Rodrigues, E. J. Dallan, M. T. Fukunaga, M. R. V. Lanza, R. R. Leme, R. C. Widner, *Brazilian J. Chem. Eng.* **1998**, *15*, 396–405.
[29] P. Jensen, S. R. Batten, G. D. Fallon, B. Moubaraki, K. S. Murray, D. J. Price, *Chem. Commun.* **1999**, *565*, 177–178.

Manuscript received: December 21, 2016
Accepted Article published: ■■ ▮▮, 0000
Manuscript revised: January 19, 2017
Final Article published: ■■ ▮▮, 0000

ARTICLES

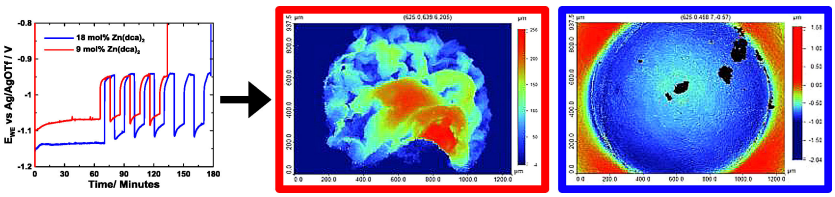

Ionic liquids for safe redox flow device? The effects of active species concentration and flow rate on the electrochemical and morphological characteristics of the Zn^{2+}/Zn^{0} redox couple are studied by using an imidazolium-based ionic liquid under a flow configuration. A superior performance can be achieved under flow configuration in terms of higher cycling efficiency and uniform deposition morphology.

*K. Periyapperuma, Dr. Y. Zhang, Prof. D. R. MacFarlane, Prof. M. Forsyth, Dr. C. Pozo-Gonzalo, Prof. P. C. Howlett**